

Electronic Mach-Zehnder interferometer in the fractional quantum Hall effect

T. Jonckheere,¹ P. Devillard,^{1,2} A. Crépieux,^{1,3} and T. Martin^{1,3}

¹Centre de Physique Théorique, Case 907 Luminy, 13288 Marseille Cedex 9, France

²Université de Provence, 13331 Marseille Cedex 3, France

³Université de la Méditerranée, 13288 Marseille Cedex 9, France

(Received 25 March 2005; revised manuscript received 15 September 2005; published 18 November 2005)

We compute the interference pattern of a Mach-Zehnder interferometer operating in the fractional quantum Hall effect. Our theoretical proposal is inspired by a remarkable experimental realization of such an interferometer with edge states in the Integer Quantum Hall effect (IQHE). The Luttinger liquid model is solved via two independent methods: refermionization at $\nu=1/2$ and the Bethe ansatz solution available for Laughlin fractions. The current differs strongly from that of single electrons in the strong backscattering regime. The Fano factor is periodic in the flux, and at $\nu=1/2$ it exhibits a sharp transition from sub-Poissonian (charge $e/2$) to Poissonian (charge e) in the neighborhood of destructive interferences. Implications for Laughlin fractions are discussed.

DOI: 10.1103/PhysRevB.72.201305

PACS number(s): 73.43.-f, 73.50.Td, 71.10.Pm

A fascinating aspect of mesoscopic physics is to build analogs of optical devices with the help of nanostructures. In many situations both phenomena can be understood with the same language.¹ However, photons propagate in vacuum and therefore interact weakly, except during their generation/detection processes. On the opposite, interactions between electrons are manifest in one-dimensional systems as well as in quantum dots. Here we want to inquire how electronic interactions affect the interference pattern of a classic optical device analog, a Mach-Zehnder (MZ) interferometer.²

Recently, such an analog was achieved with edge states of the integral quantum Hall effect (IQHE).³ Interference visibilities as high as $\sim 60\%$ were observed. Edge states of the IQHE can be understood in principle at the single electron level, but at higher magnetic fields electronic interactions are explicit in the fractional quantum Hall effect (FQHE). The latter offers the opportunity to investigate fractional charge^{4,5} and fractional statistics⁶ in one dimension. Interferometry in the FQHE was previously studied with regard to fractional charge detection⁷ using perturbation theory. Here we report on MZ interferometry using exact models: refermionization at $\nu=1/2$ (Ref. 8) and the Bethe ansatz solution.⁹ In the strong backscattering regime, the interference pattern displays a dramatic effect of the interactions; the signal is not sinusoidal, and its amplitude at the output departs from the single electron expectations.

The MZ setup³ is depicted in Fig. 1(a); an edge state is injected at voltage V_0 , and meets a quantum point contact (QPC) where it is scattered. The two resultant states recombine at a second QPC, giving two outgoing edge states 1 and 2. A magnetic field B threads the surface S enclosed by the 2 edges between the 2 QPCs, leading to an Aharonov-Bohm (AB) flux and to a corresponding phase $\Phi=SB/\Phi_0^*$, where $\Phi_0^*=hc/e^*$ is the flux quantum for excitations with fractional charge $e^*=ve$ (ν is the filling factor). This setup is topologically equivalent to the one of Fig. 1(b), 2 chiral states propagating in the same direction meeting successively two QPCs. This geometry is thus different from the simple Hall bar described in Ref. 7.

We wish to calculate the outgoing current in edge 1 and 2

for arbitrary tunneling amplitudes Γ_a, Γ_b —thus nonperturbatively—as a function of the AB phase Φ , the applied voltage $V_0=\hbar\omega_0/e^*$, the mean distance Δ between the two QPCs and the path difference δ . The AB phase is a key ingredient to the problem, as it modulates the interferences between the two paths from the first to the second QPC. As this phase is present only for cross terms with one tunneling event at QPC 1 and another at QPC 2, this amounts to multiplying the $\Gamma_a\Gamma_b^*$ terms by the phase $e^{i\Phi}$. The bosonized Hamiltonian reads (as in Ref. 8, $\hbar=e=v_F=1$, except in important results),

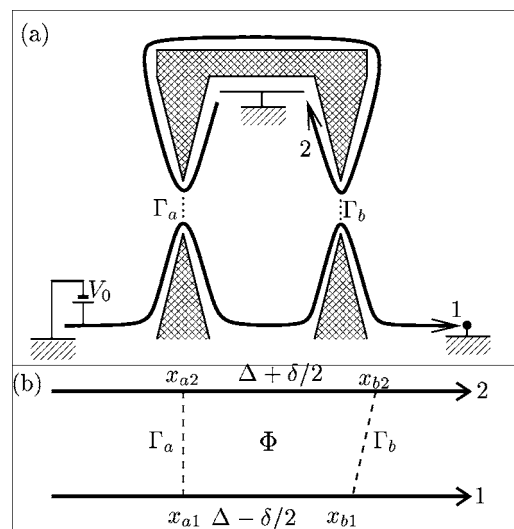


FIG. 1. (a) Mach-Zehnder geometry in the quantum Hall effect: counterpropagating edge states at a QPC are made to meet again at a second QPC. (b) Edge state configuration equivalent to (a). Γ_a (Γ_b) is the tunneling amplitude at the first (second) QPC, at $x=x_{a1}$ and $x=x_{a2}$ ($x=x_{b1}$ and $x=x_{b2}$) for edge state 1 (2). The mean distance between the two QPCs is Δ and the path difference is δ . Φ is the AB phase due to the magnetic flux.

$$H = H_{\phi_1}^0 + H_{\phi_2}^0 + \sum_{q=a,b} (\Gamma_q e^{-i\omega_0 t} e^{i\sqrt{v}[\phi_1(x_q,t) - \phi_2(x_q,t)]} + \text{H.c.}). \quad (1)$$

The first two terms in H are the free edge Hamiltonians, the next describe the tunneling of charge νe through the two QPCs. We consider the case of equal distances between the two QPCs: the first (second) QPC is located at x_a (x_b) for both edge states; unequal distances tend to reduce the interferences, but do not change the results qualitatively. Note that, as our calculations will be nonperturbative, the tunneling Hamiltonian is able to describe also electron tunneling at strong coupling, see Ref. 8.

At $\nu=1/2$, it is natural to introduce new bosonic fields $\phi_{\pm}(x) = (1/\sqrt{2})[\phi_1(x) \pm \phi_2(x)]$. The tunneling operators in Eq. (1) can be represented by a fermionic field $\eta(x) = e^{i\phi_{-}(x)}$. The Hamiltonian contains a trivial free part for ϕ_{+} , and a non-trivial part for ϕ_{-} . It is then possible to obtain a Hamiltonian which is quadratic in fermionic variables, provided that new fermionic fields are introduced such that $\psi(x,t) = \eta(x,t)f$, where f is a Majorana fermion ($f = C + C^{\dagger}$ and $\{C, C^{\dagger}\} = 1$):

$$H_{-} = \int dx \left[\psi^{\dagger}(x) (-i\partial_x - \omega_0) \psi(x) + \sum_{q=a,b} \sqrt{2\pi} \delta(x - x_q) \times [\Gamma_q \psi(x) f + \Gamma_q^{*} f \psi^{\dagger}(x)] \right]. \quad (2)$$

$\psi(x)$ is propagating in ballistically, except at $x=x_a, x_b$. The Heisenberg equations for $\psi(x,t)$ are solved by introducing plane wave solutions: $\psi(x,t) = \sum_{\omega} u_{\omega} e^{i\omega_0 x} e^{i\omega(x-t)}$, with coefficients $u_{\omega} = A_{\omega}$ (C_{ω}) for the incoming (outgoing) field at the left (right) of the two QPCs. The boundary conditions at the QPCs give

$$C_{\omega} = D^{-1} \{ [i\omega - 4\pi\tilde{\Gamma}_a \tilde{\Gamma}_b^{*} 2i \sin(\omega\Delta)] A_{\omega} - 4\pi [(\tilde{\Gamma}_a^{*})^2 + (\tilde{\Gamma}_b^{*})^2 + 2\tilde{\Gamma}_a^{*} \tilde{\Gamma}_b^{*} \cos(\omega\Delta)] A_{-\omega}^{\dagger} \}, \quad (3)$$

with $D = i\omega - 4\pi[|\Gamma_a|^2 + |\Gamma_b|^2 + (\tilde{\Gamma}_a \tilde{\Gamma}_b^{*} + \tilde{\Gamma}_a^{*} \tilde{\Gamma}_b) e^{i\omega\Delta}]$ and the tunneling amplitudes are redefined as $\tilde{\Gamma}_{a,b} = \Gamma_{a,b} e^{i\omega_0 x_{a,b}} e^{\pm i\Phi/2}$. Equation (3) can be seen as the solution of a scattering problem. Writing $C_{\omega} = r_{\omega} A_{\omega} + t_{\omega} A_{-\omega}^{\dagger}$, with reflection (r_{ω}) and transmission (t_{ω}) coefficients, one can check that the flux is conserved ($|r_{\omega}|^2 + |t_{\omega}|^2 = 1$).

From the solution Eq. (3), we can proceed to the calculation of the current I_2 outgoing in edge state 2,

$$I_2 = \frac{e}{4\pi} \int_{-\omega_0}^{\omega_0} d\omega |t_{\omega}|^2. \quad (4)$$

The outgoing current in edge state 1 is simply $I_1 = e\omega_0/(2\pi) - I_2$, where $e\omega_0/(2\pi) = \nu e^2 V_0/h$ is the incoming Hall current. It is convenient to introduce the geometric mean modulus amplitude $\Gamma = \sqrt{|\Gamma_a| |\Gamma_b|}$. The deviation from equal amplitudes is described with the parameter $\lambda (|\Gamma_a| = \lambda\Gamma, |\Gamma_b| = (1/\lambda)\Gamma)$. The transmission becomes

$$|t_{\omega}|^2 = N(u)/D(u), \quad u = \omega/(4\pi\Gamma^2),$$

$$N(u) = [(\lambda^2 + \lambda^{-2}) \cos(\omega_0\Delta + \Phi) + 2 \cos(4\pi\Gamma^2 u\Delta)]^2 + [(\lambda^2 - \lambda^{-2}) \sin(\omega_0\Delta + \Phi)]^2,$$

$$D(u) = [u - 2 \cos(\omega_0\Delta + \Phi) \sin(4\pi\Gamma^2 u\Delta)]^2 + [(\lambda^2 + \lambda^{-2}) + 2 \cos(\omega_0\Delta + \Phi) \cos(4\pi\Gamma^2 u\Delta)]^2. \quad (5)$$

The relevant regimes for observing interference fringes are either weak pinchoff ($\Gamma \rightarrow 0$) or when $(\omega_0\Delta/v_F) < 1$ at strong pinchoff. At strong pinchoff and for $(\omega_0\Delta/v_F) \gg 1$, the above integral gives $e\omega_0/(4\pi)$, and thus $I_1 = I_2 = e\omega_0/(4\pi)$, where all interferences are lost. For $(\omega_0\Delta/v_F) < 1$, the integral gives

$$I_2 \simeq (2\Gamma^2)^{\frac{1}{2}} \frac{(\lambda^2 + 1/\lambda^2) + \cos(\omega_0\Delta + \Phi)}{\frac{1}{2} - 4\pi\Gamma^2\Delta \cos(\omega_0\Delta + \Phi)} \times \tan^{-1} \left(\frac{\frac{1}{2} - 4\pi\Gamma^2\Delta \cos(\omega_0\Delta + \Phi)}{4\pi\Gamma^2 \left[\frac{1}{2}(\lambda^2 + 1/\lambda^2) + \cos(\omega_0\Delta + \Phi) \right]} \right). \quad (6)$$

Comparing this to the transmitted current for one QPC only, with tunneling amplitude Γ ,

$$I_2|_{1\text{QPC}} = 2\Gamma^2 \tan^{-1} \left(\frac{\omega_0}{4\pi\Gamma^2} \right), \quad (7)$$

we see that the current in Eq. (6) can be expressed as the current for a single QPC, with an effective tunneling amplitude Γ_{eff} ,

$$4\pi\Gamma_{\text{eff}}^2 = \frac{4\pi \left[\frac{1}{2}(|\Gamma_a|^2 + |\Gamma_b|^2) + |\Gamma_a| |\Gamma_b| \cos \Phi \right]}{\frac{1}{2} - 4\pi |\Gamma_a| |\Gamma_b| \Delta \cos \Phi}. \quad (8)$$

This is a central result: as far as the current is concerned, the MZ setup behaves, for fractionally charged excitations, as a single QPC with an effective amplitude Γ_{eff} which is modulated by the AB phase. As, in this setup which is composed of several edges, excitations are injected from one edge and are collected from another edge, we expect that the fractional statistics of these excitations play an important role in this result (see Ref. 10). Technically speaking, the difference between this behavior and the one of noninteracting electrons [as observed experimentally in the IQHE (Ref. 3)] can be traced back to the Hamiltonian. In the FQHE, the fermionic Hamiltonian of Eq. (2) couples $\psi(x,t)$ to the auxiliary fermion f for both scattering events at x_a and at x_b : these two scatterings are thus strongly linked. On the other hand, in the IQHE, the tunneling part of the Hamiltonian $H_T = \int dx \sum_{q=a,b} \delta(x - x_q) [\Gamma_q \psi_1(x) \psi_2^{\dagger}(x) + \text{H.c.}]$ couples $\psi_1(x,t)$ to $\psi_2(x,t)$ at the same location, and each QPC is described independently by a scattering matrix. This different behavior leads to dramatically different results for the interferences in the transmitted current I_2 as a function of the AB phase Φ . Consider for simplicity the case where $|\Gamma_a| = |\Gamma_b| = \Gamma$. Indeed, $\lambda=1$ merely ensures a maximum visibility for the interferences. In the IQHE, one has

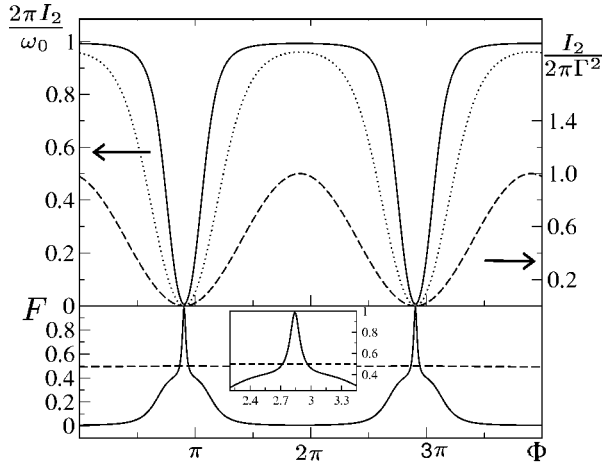


FIG. 2. Upper part: transmitted current I_2 as a function of the AB phase Φ , for 2 QPCs with $\nu=1/2$ and equal tunneling amplitudes Γ , with $\omega_0\Delta/v_F=0.3$, and $8\pi\Gamma^2/\omega_0=0.01$ (dashed curve, right y axis), 1 (dotted curve, left axis), 100 (full curve, left axis). Lower part: Fano factor $F=S_2/(2eI_2)$ as a function of Φ for the same parameters, $8\pi\Gamma^2/\omega_0=100$ (full curve), 0.01 (dashed curve, extremely narrow peaks have been removed for the sake of clarity). Inset: zoom on one of the narrow peaks of F for $8\pi\Gamma^2/\omega_0=100$.

$$I_2|_{\text{IQHE}} = \omega_0 T(1-T)[1 + \cos(\omega_0\Delta + \Phi)], \quad (9)$$

where $T=\Gamma^2/(1+\Gamma^2/4)^2$ is the transmission of each QPC, and Φ is here SB/Φ_0 ($\Phi_0=hc/e$). It shows that the maximum transmitted current in edge 2 is obtained for $T=1/2$, while it goes to 0 for $T\rightarrow 0$ ($\Gamma\rightarrow 0$) or $T\rightarrow 1$ ($\Gamma\rightarrow 2$, which is the strong coupling limit in this case). For all values of T , I_2 shows sinusoidal oscillations as a function of Φ . Considering now the results for fractionally charged excitations, Eqs. (6) and (8), one can distinguish two different regimes. First, the tunneling regime, corresponding to $\Gamma\rightarrow 0$. We have then $\Gamma_{\text{eff}}^2=2\Gamma^2[1+\cos(\omega_0\Delta+\Phi)]\ll 1$, and we recover results similar to the noninteracting case in the tunneling limit: sinusoidal oscillations of the current I_2 as a function of the AB phase Φ , with $I_2\sim\Gamma^2\ll 1$. This is easily understood: when one keeps only the lowest order in Γ , the coupling between the two scattering events disappears and the results obtained for noninteracting electrons are recovered. The opposite limit is obtained when $\Gamma\rightarrow\infty$. As shown in Fig. 2, the current I_2 is nearly constant, with the value $e\omega_0/(2\pi)$, except near $\Phi=(2n+1)\pi$ where it shows narrow dips going to zero. For very large Γ , the width of the dips scales as $\sqrt{\omega_0\Delta/v_F}<1$. This means that for large Γ , all the incoming current gets transmitted to edge 2, except for special values of the AB phase Φ where destructive interference happens. Note that this is totally different from the non interacting electron case where the incoming current in edge 1 gets scattered to edge 2 at the first QPC, then gets mostly scattered back in edge 1 at the second QPC. Because of electronic correlations, this picture is not valid in the FQHE, and the two QPCs must be considered as a whole.

The noise also has unique features. Its analytic expression is identical to that of noninteracting electrons:

$$S_2 = \frac{e^2}{2\pi} \int_{-\omega_0}^{\omega_0} d\omega |t_\omega|^2 (1 - |t_\omega|^2), \quad (10)$$

a mere consequence of the fact that the transmission in edge 2 is described by a scattering process for the reformionized field. Here, however, the energy dependence of $|t_\omega|^2$ reflects the electronic correlations. The Fano factor $F\equiv S_2/(2eI_2)$ is shown on the lower part of Fig. 2 for the two regimes discussed above. In the tunneling regime, $F\approx 1/2=\nu$: the small current outgoing in edge 2 is carried by quasiparticles of charge νe , and these can either tunnel at the first or at the second QPC. For arbitrary coupling, F is a periodic function of flux: in the regime of strong coupling, the lowering of the Fano factor is due to the factor $1-|t_\omega|^2$ in Eq. (10), when the current is close to its maximal value. When destructive interference occurs [near $\Phi=(2p+1)\pi$, p integer], I_2 is suppressed and a peculiar behavior appears. The global shape of the Fano factor suggests a value of $1/2$ (sub-Poissonian) in this region, although backscattering is strong. In the close vicinity of $\Phi=(2p+1)\pi$ there is a sharp peak, and the Fano factor reaches 1 (Fig. 2). For AB phases corresponding to this narrow peak, the noise is Poissonian, and the current is carried by pairs of quasiparticles of charge νe , here electrons. This peak is in fact present for any value of Γ , but its width decreases with Γ which makes it invisible in the small Γ limit. For the large Γ regime, and with $\omega_0\Delta/v_F\approx 0.3$, this peak could be seen if currents of a few percent of the incoming Hall current can be measured experimentally. All of the above results are robust up to $\omega_0\Delta/v_F\approx 1$; beyond this value, the visibility of the current oscillations decreases rapidly and the ‘‘Poissonian’’ peak of the Fano factor is reduced.

The chiral Luttinger liquid description is valid only for simple Laughlin fractions $\nu=1/(2p+1)$, not $\nu=1/2$. We thus have to check that our results can be observed with the experimentally accessible filling factors such as $\nu=1/3$. To this aim, we start with an imaginary time action formalism and for simplicity we consider the case $\Gamma_a=\Gamma_b=\Gamma$. Following Ref. 11, we introduce the fields $\bar{\phi}(\omega), \tilde{\phi}(\omega)=[\phi_-(x_a, \omega) \pm \phi_-(x_b, \omega)]/\sqrt{2}$. These fields are the only degrees of freedom which are left after integration of the quadratic part of the action associated with the Hamiltonian of Eq. (1). Assuming $\omega_0\Delta/v_F<1$, the effective action reads

$$\begin{aligned} \mathcal{S} = & \frac{1}{2\pi\beta} \left(\sum_{\omega} \frac{v_F}{\Delta} |\bar{\phi}(\omega)|^2 + \frac{|\omega|}{2} |\tilde{\phi}(\omega)|^2 \right) \\ & + 4\Gamma \int_0^{\hbar\beta} d\tau \cos[\sqrt{\nu}\bar{\phi}(\tau) + \Phi/2] \cos[\sqrt{\nu}\tilde{\phi}(\tau) - \Phi/2], \end{aligned} \quad (11)$$

where $\beta=1/(k_B T)$. Note that in Eq. (11), the field $\tilde{\phi}(\omega)$ is massive. For $\Delta<\hbar v_F/\Gamma$ we can neglect its fluctuations, so that the field $\tilde{\phi}(\omega)$ is pinned to zero. The leading corrections to this approximation are computed elsewhere.¹² One is then left with the field $\bar{\phi}$ only. Shifting this field by $\Phi/2$, we get a new action,

$$S = \frac{1}{4\pi\hbar\beta} \sum_{\omega} |\omega| |\phi(\omega)|^2 + 4\Gamma \cos(\Phi/2) \int_0^{\hbar\beta} d\tau \cos[\sqrt{\nu}\phi(\tau)]. \quad (12)$$

This action is identical to the zero-mass limit of the Sine-Gordon model and the problem can be solved exactly.⁹ The transmitted current I_2 follows the scaling,

$$I_2 = \frac{\nu}{2\pi} \left[c_0 \Gamma \cos\left(\frac{\Phi}{2}\right) \right]^{1/(1-\nu)} \mathcal{F} \left(\frac{\omega_0}{\nu \left[c_0 \Gamma \cos\left(\frac{\Phi}{2}\right) \right]^{1/(1-\nu)}} \right), \quad (13)$$

with $c_0 = 4\sqrt{2\pi}$. \mathcal{F} is the scaling function, with $\mathcal{F}(x) \sim x^{2\nu-1}$ for $x \gg 1$ and $\mathcal{F}(x) = x$ for $x \ll 1$. This proves that the 2 QPCs behave as 1 QPC with an effective coupling $\nu[4\sqrt{2\pi}\Gamma \cos(\Phi/2)]$ which is modulated by the AB phase. The results previously obtained for $\nu=1/2$ can therefore be extended to describe Laughlin fractions, such as $\nu=1/3$. For $\nu=1/2$, $\mathcal{F}(x)$ is simply $\tan^{-1}(x)$, and the effective coupling is $\Gamma_{\text{eff}}^2 = 8\pi\Gamma^2(1 + \cos\Phi)$. This is in agreement with Eq. (8), since by neglecting the massive field $\tilde{\phi}$ we have supposed that $\Delta \rightarrow 0$. The results for the current I_2 when $\nu=1/3$ (not shown) are in precise correspondence with those obtained for $\nu=1/2$ in the limit of $\Delta \rightarrow 0$.

Unusual features in the Fano factor (peaks near $\Phi = \pi, 3\pi, \dots$) also need to be justified for the filling factors $\nu=1/(2p+1)$. To this aim, we need to go beyond the infinite mass approximation: the scattering term in Eq. (12) is proportional to $\cos(\Phi/2)$ and is thus zero when $\Phi = \pi, 3\pi, \dots$

As the transmission is very small in this region, we perform a perturbative development to get corrections,

$$S_2 \approx \frac{\Gamma^2 \Delta}{\hbar v_F} \sin^2(\Phi/2) \int_0^{\hbar\beta} d\tau \cos[2\sqrt{\nu}\phi(\tau)]. \quad (14)$$

Although this term is not relevant for $\nu > 1/4$, it gives the main contribution to I_2 and S_2 near the Fano factor peaks where it is maximum. Because of the $\cos[2\sqrt{\nu}\phi(\tau)]$, it implies the scattering of two excitations of charge νe at once, and lead to an increase of the Fano factor from the expected ν value. Narrow peaks in the Fano factor, near $\Phi = \pi, 3\pi, \dots$ are thus to be expected for filling factors $\nu=1/(2p+1)$, as observed in the calculations at $\nu=1/2$.

To conclude, we have provided the first nonperturbative treatment of the electronic analog of an optical interferometer operating with strongly correlated fermions. The most dramatic effect occurs when both QPCs are close to pinchoff (large Γ), where the whole current exits in edge 2 (except at special values of the AB flux), contrary to the case of the IQHE and classical optics. The Fano factor is periodic in the AB phase. At strong pinchoff, at $\nu=1/2$, the noise switches from sub-Poissonian to Poissonian near the destructive AB interferences. Our predictions could be tested experimentally with the same ‘‘air bridge’’ setup as in Ref. 3. With $v_F \approx 3 \times 10^5$ m/s,¹³ the important condition $\omega_0 \Delta / v_F \leq 1$ could be reached with state of the art techniques: temperature of a few tens of mK, Δ a few μm , and V_0 a few μV .

Recently, a perturbative calculation on the same setup was presented in Ref. 14. There, Klein factors are inserted in the tunneling operators, which leads to different results.

¹See, for instance, E. Akkermans and G. Montambaux, *Physique Mésoscopique des Electrons et des Photons* (EDP Sciences, Paris, 2004).

²M. Born and E. Wolf, *Principles of Optics*, 7th ed. (Cambridge University Press, Cambridge, UK, 1999), pp. 348–352.

³Y. Ji, Y. Chung, D. Sprinzak, M. Heiblum, D. Mahalu, and H. Shtrikman, *Nature* (London) **422**, 415 (2003).

⁴C. L. Kane and M. P. A. Fisher, *Phys. Rev. Lett.* **72**, 724 (1994); C. deC. Chamon, D. E. Freed, and X. G. Wen, *Phys. Rev. B* **51**, 2363 (1995).

⁵L. Saminadayar, D. C. Glatli, Y. Jin, and B. Etienne, *Phys. Rev. Lett.* **79**, 2526 (1997); R. dePicciotto, M. Reznikov, M. Heiblum, V. Umansky, G. Bunin, and D. Mahalu, *Nature* (London) **389**, 162 (1997).

⁶R. B. Laughlin, *Rev. Mod. Phys.* **71**, 863 (1999); D. Arovas, J. R. Schrieffer, and F. Wilczek, *Phys. Rev. Lett.* **53**, 722 (1984).

⁷C. deC. Chamon, D. E. Freed, S. A. Kivelson, S. L. Sondhi, and X. G. Wen, *Phys. Rev. B* **55**, 2331 (1997); M. R. Geller and D. Loss, *ibid.* **56**, 9692 (1997).

⁸C. deC. Chamon, D. E. Freed, and X. G. Wen, *Phys. Rev. B* **53**, 4033 (1996).

⁹P. Fendley, A. W. W. Ludwig, and H. Saleur, *Phys. Rev. Lett.* **74**, 3005 (1995); *Phys. Rev. B* **52**, 8934 (1995).

¹⁰I. Safi, P. Devillard, and T. Martin, *Phys. Rev. Lett.* **86**, 4628 (2001); S. Vishveshwara, *ibid.* **91**, 196803 (2003).

¹¹A. Furusaki and N. Nagaosa, *Phys. Rev. B* **47**, 3827 (1993).

¹²T. Jonckheere, P. Devillard, A. Crépieux, and T. Martin (unpublished).

¹³C. Glatli (private communication).

¹⁴K. T. Law, D. E. Feldman, and Yuval Gefen, cond-mat/0506302 (unpublished).